Hindawi Publishing Corporation
International Journal of Antennas and Propagation
Volume 2015, Article ID 864327, 11 pages
http://dx.doi.org/10.1155/2015/864327

Research Article

BDS Multipath Parameter Estimation in the Presence of Impulsive Noise

Jicheng Ding, Lin Zhao, Chun Jia, and Zhibin Luo

College of Automation, Harbin Engineering University, Harbin 150001, China

Correspondence should be addressed to Jicheng Ding; aaron.heu@163.com

Received 25 September 2014; Accepted 18 January 2015

Academic Editor: Ding-Bing Lin

This study focuses on mitigating the multipath, especially the short-delay multipath of the BeiDou navigation satellite system under impulsive noise conditions. A modified least mean p-norm (LMP) algorithm is developed to reduce the convergence time with the same steady-state error by predicting the updating trend of weights. The modified normalized power and the normalized polynomial least mean pth power are also directly provided according to a similar principle. According to the research work, an average filter has been utilized to improve the processing gain of designed mitigation scheme. Some significant simulation results verified the performance of the proposed adaption algorithm. Multipath parameter estimation tests have been conducted under different noise levels. Some comparative statistics performance assessments are quantified and verified under impulsive and additional white Gaussian noise environments. Results with various window widths of the average filtering and carrier-to-noise ratios indicate that the proposed scheme is able to improve the performance of the short-delay multipath mitigation under normal and degraded environments.

1. Introduction

The BeiDou navigation satellite system (BDS), which currently covers the Asia Pacific region, is aimed at entering the global network stage and becoming a global navigation satellite system (GNSS) in 2015. The BDS will eventually operate in the ocean, urban, and indoor environments, similar to the global positioning system (GPS) [1].

The multipath problem has received considerable attention in recent years as the dominant error source in the preceding applications. Traditional techniques suffer from a common drawback in their ineffectiveness to suppress short-delay multipath signals (i.e., less than approximately 20 m) with respect to the line-of-sight (LOS) signal [2]. This situation is a big limitation because the real-life multipath tends to be the close-in, short-delay type. The a posteriori multipath estimation (APME) [2], swarm intelligence optimization algorithms [3], and adaptive filtering techniques [4, 5] are the approaches used to suppress the short-delay multipath. The APME has improved in order to suppress the short-delay multipath signal, but its rejection of the medium-delay multipath is unsatisfactory. The swarm intelligence optimization method is difficult to be implemented for practical applications because of its computational complexity. The adaptive filtering method is a practical technology which includes the recursive least squares (RLS) adaptive filtering algorithm and is mostly based on Gaussian assumptions. The RLS using the minimum mean square error criterion completes the inverse and iterative adaptive operation by using a simplified matrix and provides a small steady-state error. Accordingly, the limitations of the RLS are defined by the optimal assumptions. This condition ensures an analytical solution for the detection of a known signal in additional white Gaussian noise (AWGN) [4–6] in most cases.

The GNSS signal is buried in noise due to limitedly transmitted power from the satellites. Some effective algorithms mostly are based on the signal despreading to obtain enough processing gain. Compared with the signal-to-noise ratio (SNR), the carrier-to-noise ratio (CNR) is more easily accepted by lots of literatures to assess the performance of a GNSS receiver. It is defined according to the noise power in a 1 Hz bandwidth. In fact, in the context of digital modulations,

digitally modulated signals are usually referred to as carriers. Therefore, the term CNR, instead of SNR, is preferred to express the signal quality when the signal has been digitally modulated. Moreover, the traditional adaptive filter has to be applied before the signal despreading, which leads to a limited processing gain. However, this problem has apparently not been discussed in [4–7].

As mentioned previously, the growing need for indoor GNSS and the increasing demand for satellite-based navigation in manned and autonomous ground, aerial, and surface vehicles have to be addressed. Hence, the GNSS receivers are operated in close proximity to various noise sources with Gaussian and non-Gaussian characteristics. Such non-Gaussian random signals contain a large number of outliers. These outliers disturb the receiver's performance by impeding the baseband signal processing phase and increase the ranging error and bit error rates [8]. References [8–11] have thoroughly analyzed these non-Gaussian impulsive sources and the effect on the receiver, which operates in the GNSS operating band. For instance, the impulsive signal source is the ultra-wideband signals which cover the GNSS operating band and are adopted more and more in outdoor and indoor environments. The model for these signals cannot be justified because of the Gaussian noise. Accordingly, an important class of distributions (i.e., a-stable distributions) is used to model this type of impulsive noises [11–14].

In order to overcome these problems, many variations of the least mean squares (LMS) have been proposed over the past decades. These LMS methods include the variable step-size approach [15], the affine projection algorithms [16], and the higher- or lower-order statistics method [17]. The third method yields many robust algorithms with improved convergence rate and robustness against the impulsive interference. The higher- or lower-order statistics method includes the least mean p-norm (LMP) and its normalized version (NLMP algorithm), which have been reported in [17, 18]. Additionally, [19] has proposed the normalized polynomial least mean pth power (NPLMP) to improve the algorithm convergence rate by extending the LMP algorithm. Moreover, some variable step-size sign algorithms similar to the extended LMS are also effective to accelerate the convergence process [20]. This study introduces another method to accelerate the LMP algorithm convergence process by using a self-tuned weighted term, which is an extension from other classic algorithms.

The structure of the paper is as follows. In Section 2, a BDS multipath parameter estimation scheme based on adaptive filter with an average filter is designed. Section 3 presents the derivation and analysis of the modified LMP adaptive filter and some extended algorithms which use the self-tuned weighted term. A variety of comparable tests are conducted in Section 4. The interesting results and analysis are also presented in this section. The conclusions are provided in Section 5.

2. BDS Multipath Parameter Estimation

2.1. BDS B1 Signal Model in Multipath Environments. The description of the statistical model of the received signal in the presence of a multipath is difficult in the case of a BDS. Nevertheless, many hypotheses are made. One of these hypotheses assumes that the multipath signals are delayed with respect to the direct BDS signal. The reflected signals with a delay of less than one chip will usually be considered because the signals with a code delay which is larger than one chip are uncorrelated with the direct signals; otherwise, the multipath signal is assumed to have lower power than the direct one. The baseband signal model is represented as follows:

$$s_{\mathrm{IF}}(n) = \sum_{m=0}^{M} A_m C\left(nT_s - \tau_m\right) e^{j(2\pi f_{\mathrm{IF}} nT_s + \theta_m)} + \eta_{\mathrm{IF}}(n), \quad (1)$$

where $m = 0$ represents the LOS component; $C(\cdot)$ is the ranging code, which modulates the Neumann-Hoffman code; T_s is the sampling period; f_{IF} is the immediate frequency; η_{IF} is the noise; and A_m, τ_m, and θ_m are, respectively, the amplitude, carrier phase, and code delay of the mth delay component.

Unlike GPS signals, the NH code period is selected according to the duration of a navigation data bit [21]. The bit duration of the NH code is equal to bit period of the ranging code. The duration of one navigation data bit is 20 ms, while that of the ranging code is 1 ms (Figure 1). The NH code (0, 0, 0, 0, 0, 1, 0, 0, 1, 1, 0, 1, 0, 1, 0, 0, 1, 1, 1, 0) with a length of 20 bits, a rate of 1 kbps, and a bit duration of 1 ms is synchronously modulated on the ranging code with the navigation data bit.

As described in Section 1, if the η_{IF} is impulsive noise, the a-stable distribution is able to be used to model this type of noises. Its characteristic function has the following form [17]:

$$\varphi(t) = \exp\left(jat - \gamma|t|^{\alpha}\left[1 + j\beta\,\mathrm{sign}(t)\,\omega(t,\alpha)\right]\right), \quad (2)$$

where $-\infty < a < +\infty$, $\gamma > 0$, $0 < \alpha \le 2$, $-1 \le \beta \le 1$ and

$$\omega(t,\alpha) = \begin{cases} \tan\left(\dfrac{\alpha\pi}{2}\right) & \alpha \ne 1 \\ \left(\dfrac{2}{\pi}\right)\log|t| & \alpha = 1. \end{cases} \quad (3)$$

a is location parameter, γ is scale parameter, also called the dispersion, β is index of skewness. α is characteristic exponent.

The characteristic exponent α is a shape parameter. It measures the "thickness" of the tails of the density function. α values close to 0 indicate impulsive nature that is considerable probability mass in the tails of the distribution. α values close to 2 indicate a more Gaussian type of behavior. When $\beta = 0$, the distribution is symmetric about the center a. Symmetric stable distributions with characteristic exponent α are called symmetric α-stable (SαS). The dispersion γ can be any positive number and behaves like the variance. When $\alpha = 2$, it is half of the variance.

2.2. Error Analysis of the BDS Code Discriminator. Considering an early-minus-late power code discriminator, three pairs of correlators are required to produce three in-phase components (i.e., I_E, I_P, and I_L) and three quadraphase components (Q_E, Q_P, and Q_L). These components, respectively, correspond to the early (E), punctual (P), and late (L) reference

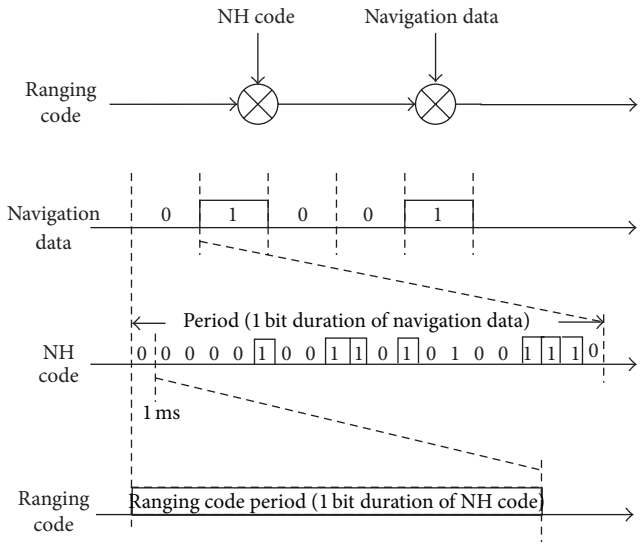

Figure 1: BDS CBII NH code modulation.

ranging codes. The discriminator's output is expressed as follows [8]:

$$\begin{aligned} D &= \left(I_E^2 + Q_E^2\right) - \left(I_L^2 + Q_L^2\right) \\ &= \left(\sqrt{ST}R(\tau_E)\cos\phi + \eta_{I_E}\right)^2 + \left(\sqrt{ST}R(\tau_E)\sin\phi + \eta_{Q_E}\right)^2 \\ &\quad - \left(\sqrt{ST}R\left(\tau_L\right)\cos\phi + \eta_{I_L}\right)^2 \\ &\quad - \left(\sqrt{ST}R\left(\tau_L\right)\sin\phi + \eta_{Q_L}\right)^2, \end{aligned} \tag{4}$$

where S is the signal power; T is the loop integration time, which is usually equal to the ranging code period; R is the cross-correlation function between the incoming ranging code and the reference code; ϕ is the residual phase error; and $\eta_{I_E}, \eta_{Q_E}, \eta_{I_L}, \eta_{Q_L}$ are the in-phase and quadraphase noise components of the correlator outputs.

Zero is an expected result for (4) assuming that d_c is the early-late correlator spacing. The tracking error ρ is then obtained by applying the derivation process in [8] as follows:

$$\begin{aligned} \rho = \tau_P\big|_{D=0} &= \frac{\eta_{I_E}^2 + \eta_{Q_E}^2 - \eta_{I_L}^2 - \eta_{Q_L}^2}{8ST\left(1 - d_c/2\right)} \\ &\quad + \left(\left(\sqrt{2ST}\left(1 - \frac{d_c}{2}\right)\right.\right. \\ &\qquad \left.\left. \cdot \left[\left(\eta_{I_E} - \eta_{I_L}\right)\cos\phi + \left(\eta_{Q_E} - \eta_{Q_L}\right)\sin\phi\right]\right) \\ &\qquad \cdot \left(2ST\left(1 - \frac{d_c}{2}\right)\right)^{-1}\Bigg). \end{aligned} \tag{5}$$

The code tracking error is proportional to the integration time T and inversely proportional to the early-late correlator spacing d_c.

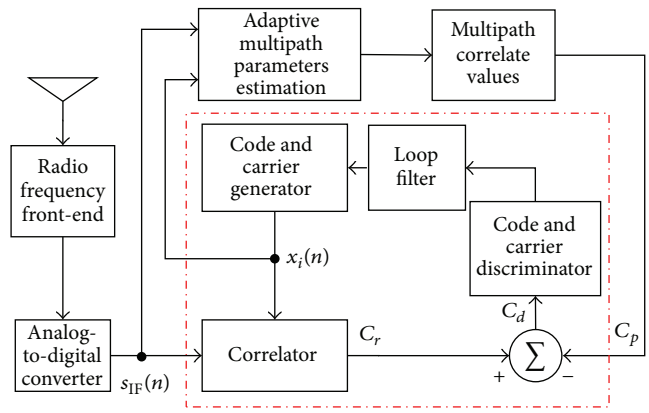

Figure 2: Multipath mitigation scheme.

The generalized central limit theorem is one of the important characteristics of the α-stable distribution. Therefore, an average filter is considered to further suppress the noise according to (5) and improve the processing gain. Its basic principle is that a sliding window is set in a working region of a function and the average of all elements in the window is at the center of the window. Accordingly, time domain filtering is carried out. The average filter adjusts the relevant parameters of the large pulse and weakens their influence, thereby reserving the useful signal components.

2.3. Modified BDS Multipath Mitigation in the Presence of Impulse Noise. The adaptive multipath suppression scheme in the presence of impulsive noise is shown in Figure 2 [4–6]. The modules in the dotted box are a classic signal tracking loop. The input of the adaptive multipath parameter estimation is the received digital intermediate frequency signal, the local code, and the carrier numerically controlled oscillator output.

2.3.1. Multipath Parameter Estimation. The adaptive filter module identifies the direct and multipath signal using adaption algorithm. The multipath signal amplitude is then estimated from the output weights. The delay elements corresponding to the amplitude are also obtained.

2.3.2. Tracking Error Compensation. The impact of the correlation value C_m of the mth multipath signal to the correlation value C_r of the received signal is obtained from the ranging code autocorrelation function according to the estimated amplitude, propagation delay of the multipath, relative phase of the reference signal, and autocorrelation function of the ranging codes.

2.3.3. Mitigation Multipath Effects. The correlation value C_r of the received signal subtracts superposition $C_p = \sum C_m$ of all of the correlation values of the multipath signals, with the result as $C_d = C_r - C_p$. C_d is similar to the code discriminator input.

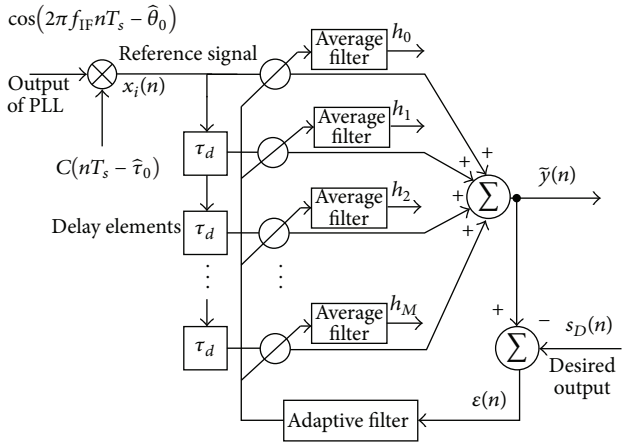

Figure 3: Proposed weight updating process.

The reference signal in this scheme has not been despread before the multipath parameter estimation. Hence, its processing gain is very low because of the low GNSS signal receive power (i.e., typically −130 dBm). Moreover, the RLS adaption algorithm is usually used for parameter estimation. Some deficiencies also exist when a GNSS receiver works in the presence of an impulsive noise environment.

In this paper, a design based on the modified adaption algorithm with self-tuned weight was used to suppress the multipath in the impulsive noise environment, to improve the processing gain of the system, and to reduce the ambient noise (Figure 3). Furthermore, an average filter with a window is also introduced to improve the processing gain.

Parameter τ_d is the minimum delay unit in Figure 3.

Assuming that $\widehat{A}_m$, $\widehat{\tau}_m$, and $\widehat{\theta}_m$ are the amplitude estimation of the weight coefficient h_m, delay estimation, and phase error estimation $\arg(h_m)$ for the mth delay element, respectively, the local carrier demodulates the received intermediate frequency signal $s_{\mathrm{IF}}(n)$ as follows:

$$s_D(n) = \sum_{m=0}^{M} A_m C\left(nT_s - \tau_m\right) \exp\left(j\left(\theta_m - \widehat{\theta}_0\right)\right) + \eta'(n), \tag{6}$$

where η' is the noise after removing the carrier component.

Restructuring signal $r_0 = \mathrm{NH}(nT_s + \widehat{\tau}_0) C(nT_s + \widehat{\tau}_0)$, obtain a time delay as follows:

$$r_m = \mathrm{NH}\left(nT_s + \widehat{\tau}_0 - mT_s\right) C\left(nT_s + \widehat{\tau}_0 - mT_s\right) \quad (m = 0, 1, \ldots, M). \tag{7}$$

When $\tau_d = T_s$, the filter output is expressed as follows:

$$\widetilde{y}(n) = \sum_{m=0}^{M} h_m C\left(nT_s + \widehat{\tau}_0 - mT_s\right). \tag{8}$$

An error signal $\varepsilon(n)$ is obtained by comparing the desired signal $s_D(n)$ with the filter output $\widetilde{y}(n)$. The error signal is used to adjust the adaptive filter weights. The average filter is adopted after the weights convergence to obtain a higher processing gain. The relationship of the weights and the parameters of $s_D(n)$ is described as follows.

If $\tau_0 - \widehat{\tau}_0 = 0$, then

$$h_0 = A_0 \exp j\left(\theta_0 - \widehat{\theta}_0\right). \tag{9}$$

If $\tau_m - \widehat{\tau}_0 = mT_s$, then

$$h_m = A_m \exp j\left(\theta_m - \widehat{\theta}_m\right). \tag{10}$$

3. Least Mean p-Norm Algorithm Using Self-Tuned Weight

The adaptive linear system model is expressed as

$$y(k) = \mathbf{w}^{\mathrm{T}}(k)\,\mathbf{x}(k), \tag{11}$$

where $\mathbf{w}(k) = [w_1(k), w_2(k), \ldots, w_N(k)]^{\mathrm{T}}$ is the weight vector, $\mathbf{x}(k) = [x_1(k), x_2(k), \ldots, x_N(k)]^{\mathrm{T}}$ is the input vector, $y(k)$ is the output, N is the order of the adaptive filter.

Assuming that the ideal system output is $d(k)$, the output error is

$$e(k) = d(k) - y(k). \tag{12}$$

By using $E[|e(k)|^p]$ instead of the mean square error (MSE) of LMS, the weight update rule of the traditional LMP algorithm is obtained as [17]

$$\mathbf{w}(k+1) = \mathbf{w}(k) + \mu |e(k)|^{p-1} \mathbf{x}(k) \operatorname{sign}(e(k)), \tag{13}$$

where μ is the step size.

A self-tuned weight update process is to improve the convergence of the LMP algorithm, and the convergence is accelerated by introducing weight trends.

Given a cost function

$$J(\mathbf{w}, k) = \sum_{i=1}^{k} \lambda^{k-i} \left|d(i) - y(i)\right|^p, \tag{14}$$

where λ is an exponent weight factor and $0 < \lambda < 1$.

Calculate the gradient of the function $J(\mathbf{w}, k)$ at $\mathbf{w}$ to obtain an instantaneous gradient estimation which is

$$\nabla_w J(\mathbf{w}, k) = p \sum_{i=1}^{k} \lambda^{k-i} |e(i)|^{p-1} \mathbf{x}(i) \operatorname{sign}(e(i)). \tag{15}$$

Applying the gradient search, obtain the coefficient update rule, which is

$$\begin{aligned} \mathbf{w}(k+1) &= \mathbf{w}(k) + \frac{\mu}{p} \nabla_w J(\mathbf{w}, k) \\ &= \mathbf{w}(k) + \mu \sum_{i=1}^{k} \lambda^{k-i} |e(i)|^{p-1} \mathbf{x}(i) \operatorname{sign}(e(i)) \\ &= \mathbf{w}(k) + \mu |e(t)|^{p-1} \mathbf{x}(k) \operatorname{sign}(e(k)) \\ &\quad + \mu \sum_{i=1}^{k-1} \lambda^{k-i} |e(i)|^{p-1} \mathbf{x}(i) \operatorname{sign}(e(i)). \end{aligned} \tag{16}$$

By (15) and (16), the previous weight update rule is replaced by $k-1$ after making k. Some necessary arrangements are expressed as

$$\begin{aligned}\mathbf{w}(k) &= \mathbf{w}(k-1) + \frac{\mu}{p}\nabla_w J(\mathbf{w}, k-1) \\ &= \mathbf{w}(k-1) + \mu\sum_{i=1}^{k-1}\lambda^{k-1-i}|e(i)|^{p-1}\mathbf{x}(i)\operatorname{sign}(e(i)) \\ &= \mathbf{w}(k-1) + \frac{\mu}{\lambda}\sum_{i=1}^{k-1}\lambda^{k-i}|e(i)|^{p-1}\mathbf{x}(i)\operatorname{sign}(e(i)).\end{aligned} \tag{17}$$

The following relationship is carried out according to (17):

$$\begin{aligned}&\sum_{i=1}^{k-1}\lambda^{k-i}|e(i)|^{p-1}\mathbf{x}(i)\operatorname{sign}(e(i)) \\ &\quad= \frac{\lambda}{\mu}(\mathbf{w}(k) - \mathbf{w}(k-1)).\end{aligned} \tag{18}$$

Substituting (18) to (16), obtain the following equation:

$$\begin{aligned}\mathbf{w}(k+1) &= \mathbf{w}(k) + \mu|e(k)|^{p-1}\mathbf{x}(k)\operatorname{sign}(e(k)) \\ &\quad+ \lambda(\mathbf{w}(k) - \mathbf{w}(k-1)).\end{aligned} \tag{19}$$

Apply similar derivation and denote $\Delta\mathbf{w}_n = \mathbf{w}(k) - \mathbf{w}(k-n)$. Accordingly, a new weight updating rule was obtained:

$$\begin{aligned}\mathbf{w}(k+1) &= \mathbf{w}(k) + \mu|e(k)|^{p-1}\mathbf{x}(k)\operatorname{sign}(e(k)) \\ &\quad+ \frac{\Delta\mathbf{w}_n}{(1/\lambda^n + \cdots(1/\lambda^2) + 1/\lambda)} \\ &= \mathbf{w}(k) + \mu|e(k)|^{p-1}\mathbf{x}(k)\operatorname{sign}(e(k)) \\ &\quad+ \frac{(1-\lambda)\lambda^n}{1-\lambda^n}\Delta\mathbf{w}_n.\end{aligned} \tag{20}$$

The weight updating process in the modified LMP (MLMP) algorithm is shown in (20). According to its derivation process, we can infer the following.

(1) The weight vector will be convergent when (14) reaches the minimum, which is the weighted average p-norm.

(2) n can be any integer value and should be larger or equal to zero for the additional term $(((1-\lambda)\lambda^n)/(1-\lambda^n))\Delta\mathbf{w}_n$ in (20). This value is used to accelerate the convergence speed as an additional weight-changing tendency. If n is equal to zero, it will be similar to the well-known LMP algorithm.

(3) If parameter n is a constant, a faster convergence will be achieved with a greater λ.

Further conclusion will be determined by comparing (20) with (13), which represents the classic LMP algorithm. The initial aim of the idea is to predict the weight updating tendency at a current time using the prior results. If a larger n is adopted while λ is set to a constant, the last term will not reflect the weight updated tendency at the current time considering $\lim_{n\to\infty}(((1-\lambda)\lambda^n)/(1-\lambda^n))\Delta\mathbf{w}_n \to 0$. Furthermore, the algorithm will be gradually reduced to the well-known LMP algorithm. On the other hand, parameter λ should not be too large if n is set to a certain constant; otherwise, the weight-changing tendency will be overestimated. In contrast, the weight-changing tendency will be underestimated when λ is too small. As a result, the algorithm convergence will not be significantly improved.

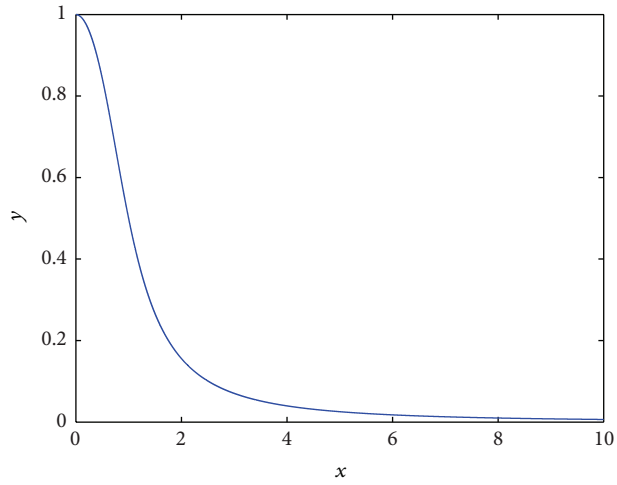

Figure 4: $y = (2/\pi)\text{arctg}(x)$.

A larger λ is expected to be used in order to speed up the weight convergence before the algorithm reaches the convergence status. Moreover, λ should be quickly decreased to zero when the algorithm begins to converge. The initial weight value is usually set to zero to meet the preceding requirement. As a result, this study uses an arctan function to adjust λ because of its particular profile (Figure 4).

The following rule is applied to ensure that λ is equal to zero after the weights arrive at its convergence:

$$\lambda(k) = \begin{cases}\dfrac{2}{\pi}\text{arctg}\left(\dfrac{1}{\|\mathbf{w}(k)\|^2}\right) & k < N \\ 0 & k \geq N,\end{cases} \tag{21}$$

where N is determined by adjusting time of weights.

To improve the convergence properties of LMP, two well-known normalized adaptation algorithms, NLMP and NPLMP, with the motivation of the normalized-LMS algorithm have been derived based on LMP. These two adaptation algorithms have the following time update [18, 19], respectively.

NLMP:

$$\mathbf{w}(k+1) = \mathbf{w}(k) + \frac{\mu|e(k)|^{p-1}\operatorname{sgn}(e(k))}{\|\mathbf{y}(k)\|_p^p + \delta}\mathbf{y}(k). \tag{22}$$

NPLMP:

$$\mathbf{w}(k+1) = \mathbf{w}(k) + \frac{\mu p|e(k)|^{p-1}\operatorname{sgn}(e(k))}{\|\mathbf{y}(k)\|_p^p + \delta}\mathbf{y}(k). \tag{23}$$

In (22) and (23), normalization is obtained by dividing the update term by the p-norm of the input vector, $\mathbf{y}(k)$. The regularization parameter δ is used to avoid excessively large updates in case of an occasionally small input.

Similar to the MLMP derived in (20), the following new weight updating rules would be, respectively, obtained when the principle above is extended to NLMP and NPLMP algorithms.

MNLMP:

$$\mathbf{w}(k+1) = \mathbf{w}(k) + \frac{\mu |e(k)|^{p-1} \operatorname{sgn}(e(k))}{\|\mathbf{y}(k)\|_p^p + \delta}\mathbf{y}(k) + \frac{(1-\lambda)\lambda^n}{1-\lambda^n}\Delta\mathbf{w}_n. \tag{24}$$

MNPLMP:

$$\mathbf{w}(k+1) = \mathbf{w}(k) + \frac{\mu p |e(k)|^{p-1} \operatorname{sgn}(e(k))}{\|\mathbf{y}(k)\|_p^p + \delta}\mathbf{y}(k) + \frac{(1-\lambda)\lambda^n}{1-\lambda^n}\Delta\mathbf{w}_n. \tag{25}$$

4. Test Results and Analysis

4.1. Comparative Performance Analysis for Least Mean p-Norm Algorithm with Self-Tuned Weight. The following are the AR(2) α-stable processes considered in the simulation studies:

$$x(n) = a_1 x(n-1) + a_2 x(n-2) + u(n), \tag{26}$$

where $a_1 = 0.97$, $a_2 = -0.7$ are the coefficients of the AR(2) process. $u(n)$ is an α-stable sequence of independent and identically distributed random variables. Its mathematical model has been described in (2). The common distribution of $u(n)$ is an even function, that is, $\beta = 0$ in (2). The characteristic exponent α is set to 1.5. The dispersion γ is set to one to avoid the loss of generality. It should be pointed out that the γ is used to adjust CNR in Section 4.2 due to its variance behavior.

Two sets of simulation studies are performed. The step size μ is set to 0.001 in the first set. The tap weight adaptation is performed for the LMP and MLMP algorithms with $n = 1, 5, 10, 20$. The N is set to 2000 in (21). The transient behaviors of the tap weight adaptations for the AR(2) process are plotted in Figure 5. Correspondingly, the introduced MLMP has a better convergence behavior than the traditional LMP algorithm.

A smaller n results in faster convergence rate for the MLMP algorithm (Figure 5). The convergence time can be reduced to 1000 from 3000 iterations when n is equal to 1. The MLMP algorithm only needs to calculate the weight trend term and store the weight value of the previous time. The computation burden slightly increases because of its recursive implementation structure. Furthermore, the advantage of the algorithm gradually weakens when the value of n becomes larger. This phenomenon is explained in Figure 6. A smaller

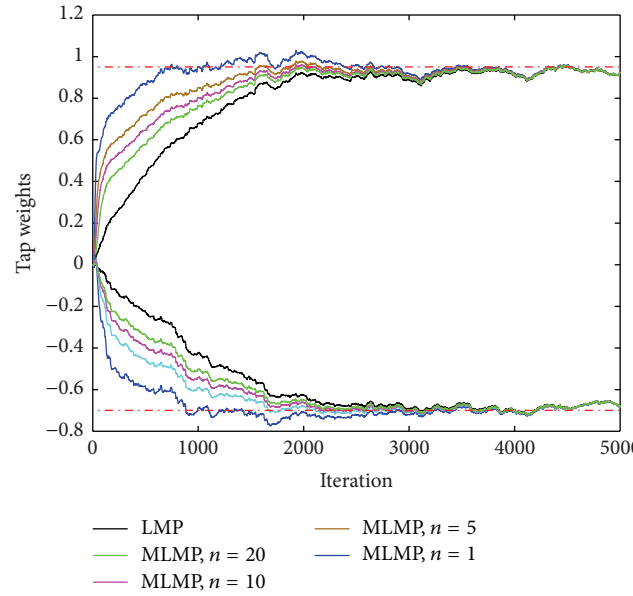

Figure 5: Weight convergence history for different n.

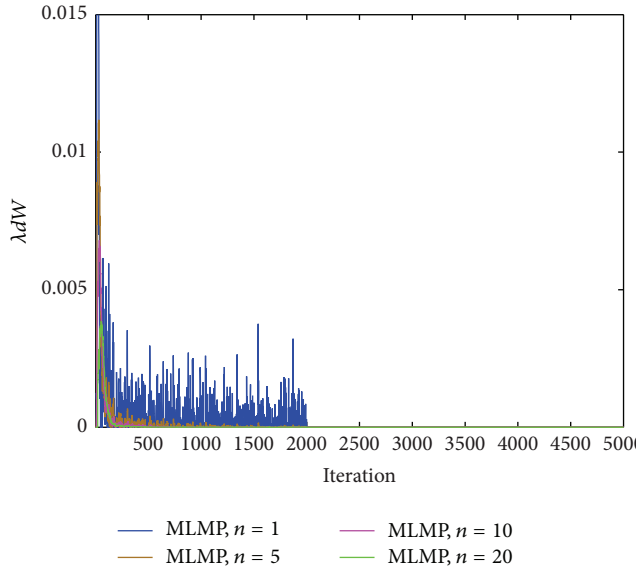

Figure 6: Corresponding predicted weight variation tendency.

value of n during the weight-adjusting process results in the prediction of more significant effects of the weight-changing tendency.

The second simulation tests the performances of the LMP (13), MLMP (20), NLMP (22), MNLMP (24), NPLMP (23), and MNPLMP (25) algorithms when n is equal to 1. The adaptation performances are plotted in Figures 7 and 8 using 100 Monte Carlo trials of the experiment. The three new weight updating approaches have comparable performances. Accordingly, they converge faster than the traditional weight updating approaches. Their final estimation error is similar to the traditional approaches, where $E(k) = \|\underline{w(k)} - \underline{w^*}\|$, $\underline{w(k)}$,

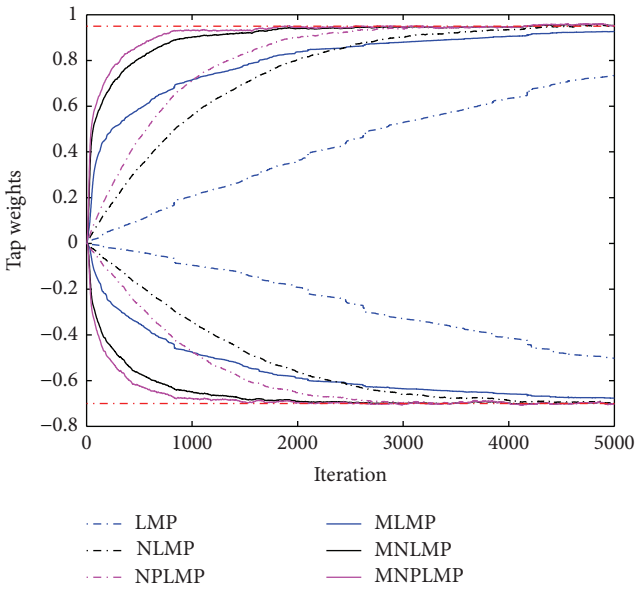

Figure 7: Weight convergence history of different approaches.

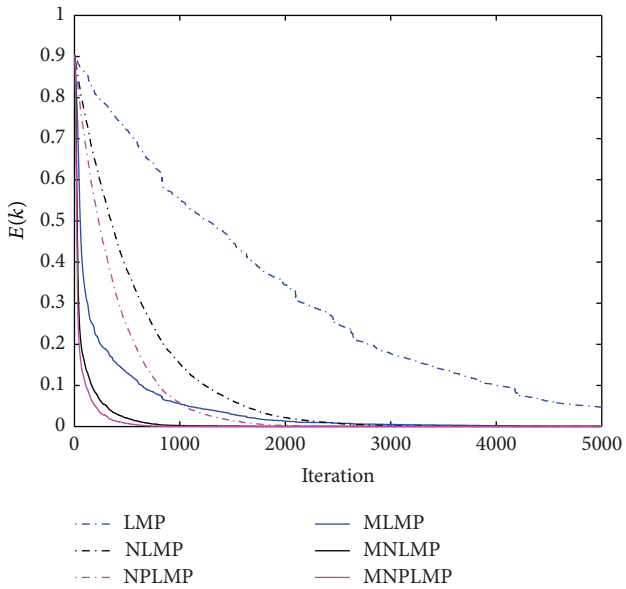

Figure 8: Corresponding stable error history curve.

and $\underline{w}^*$ are the current tap weight and the optimal solution vectors, respectively (Figure 8).

Because the MNPLMP has a faster convergence rate than the MLMP and MNLMP algorithms, the MNPLMP algorithm has been used in the following tests.

4.2. Multipath Parameters Estimation Performance. After evaluating the convergence performance of the improved adaption algorithm under different conditions in Section 4.1, this section focuses on evaluating the proposed BDS multipath parameter estimation scheme. The scheme based on the RLS algorithm is widely accepted. Additionally, [6] provides a detailed comparison of the RLS adaptive multipath mitigation method based on the traditional narrow correlator. Correspondingly, the multipath delay lock loop, the Strobe correlator, and the RLS adaptive multipath mitigation method in the long- and short-delay multipath aspects are significantly advantageous. Therefore, a comparison of the MNPLMP and RLS mitigation schemes is conducted in this section. The same average filter has also been added to the tested RLS scheme to increase the processing gain. It is different from previous studies (e.g., [4–7]).

The following settings are employed in the simulation tests: a software simulator generates the tested BDS B1 signal with an IF frequency of 4.092 MHz and a sampling frequency of 16.368 MHz; the code correlator spacing is half of a chip; and the front-end filter bandwidth is 4.5 MHz. Three multipath signals are added into the LOS according to (1). Their amplitudes and delay relation to the LOS are $A_1 = 0.3$, $\tau_1 = T_c/8$; $A_2 = 0.5$, $\tau_2 = 3T_c/8$; and $A_3 = 0.6$, $\tau_3 = T_c/2$. The corresponding code and the carrier phase delay are calculated using these parameters. Obviously, the first component is a short-delay.

The following three simulations were set up to evaluate the performance of the proposed scheme: the effective test of the average filter, the estimation performance in various CNRs, and the time delay estimation. Moreover, in addition to the impulsive noise, the AWGN noise environments are also tested considering realistic application scenarios. The various CNRs are calculated based on signal power and the dispersion γ for impulsive noise environments, and AWGN variance is used for AWGN noise environments.

The coordinate scale of the test results obtained from the two different schemes varies greatly, especially for the impulsive noise. As a result, a separate display for the test results of the MNPLMP and RLS mitigation schemes is provided to observe the details better.

4.2.1. Effective Test of the Average Filter. The window width of the average filter is increased from 1 ms to 20 ms, and the maximum is determined by the navigation data period. The estimated amplitudes are obtained by 100 independent trials of the experiment. A different computer realization of the noise is rendered for each trial. The mean and the variance of the amplitude estimation errors under the impulsive noise environment are shown in Figure 9. Figures 9(a) and 9(b) illustrate the MNPLMP and the RLS algorithms, respectively. The expected behaviors of the MNPLMP scheme have been plotted in the figure, especially in terms of the wide window of the average filter and the smaller mean and variance of the estimation error. The short-delay component has been correctly estimated. The third multipath has a more significant delay, which has achieved more estimation precision. Steady estimation results are obtained for all of the three multipath signals when the window width of the average filter is more than 10 ms. Meanwhile, the test results for the RLS scheme are unacceptable even using the 20 ms window width.

The test results for the two schemes under the AWGN environment are shown in Figure 10. Both schemes obtain a small estimation error, and the precision is similar.

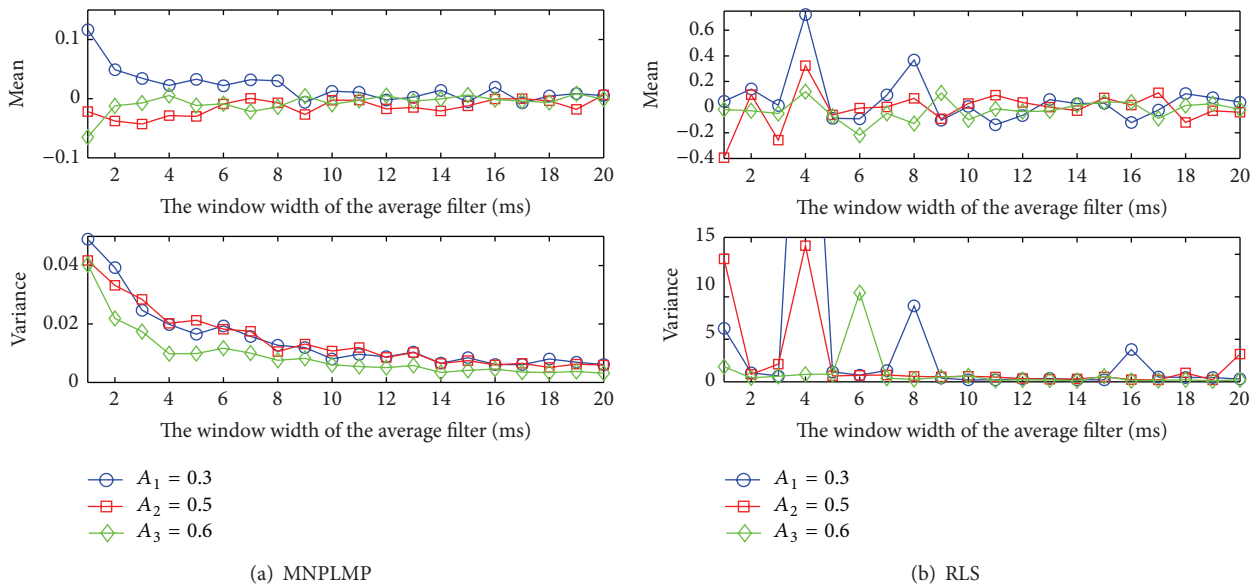

Figure 9: Multipath amplitude estimation error in various average filtering times under the impulsive noise environment.

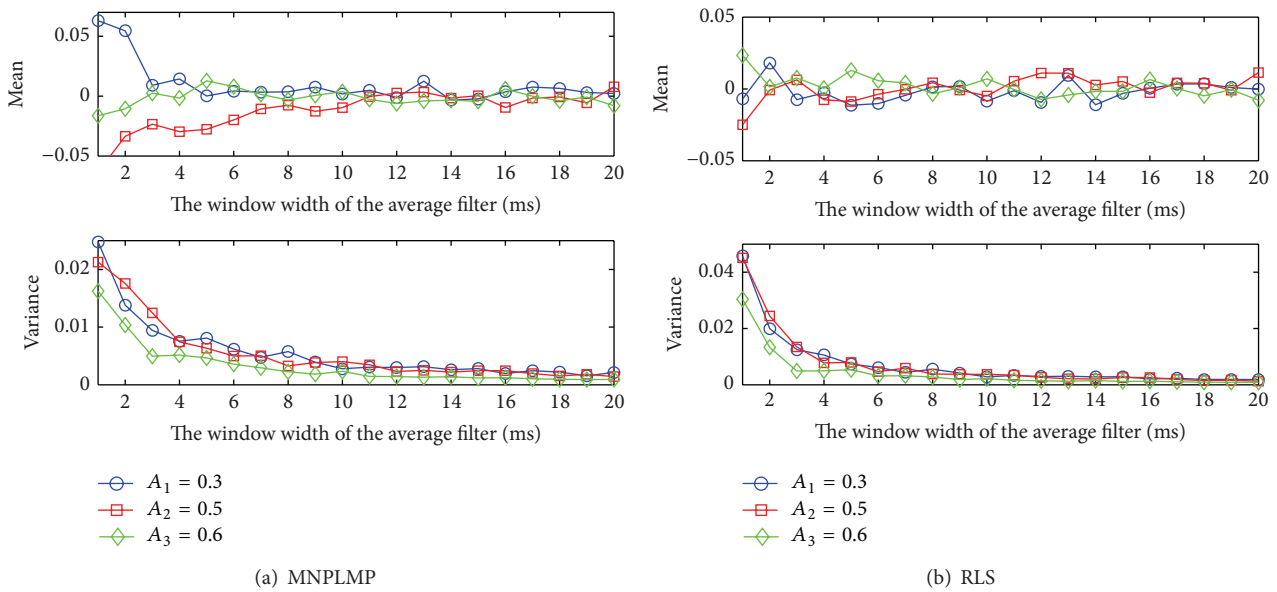

Figure 10: Multipath amplitude estimation errors in various average filtering times under the AWGN environment.

4.2.2. Amplitude Estimation Errors to Various CNRs. The window width of the average filter is set to 20 ms to assess the estimation error under various CNRs. The range of the tested CNR is 25–45 dB-Hz although 45 dB-Hz has been used on the previous experiment. The received signal quality on the light indoor and open sky condition is actually in this range. Similarly, 100 independent trials of the experiment have been conducted.

The mean and the variance of the amplitude estimation error are plotted in Figure 11. The obtained estimation error using the MNPLMP scheme gradually becomes smaller when the tested CNR increases. Furthermore, the acceptable performance is obtained for the CNRs greater than 35 dB-Hz. The RLS scheme is also unstable even in high CNR conditions.

Figure 12 shows the very similar results under the AWGN noise conditions.

4.2.3. Delay Estimation Test Results and Analysis. The delay recognition capability of the algorithm in different settings was valued. The CNR was set to 40 dB-Hz; the delay range was gradually increased from 0.125 chips to 1.5 chips by 0.125

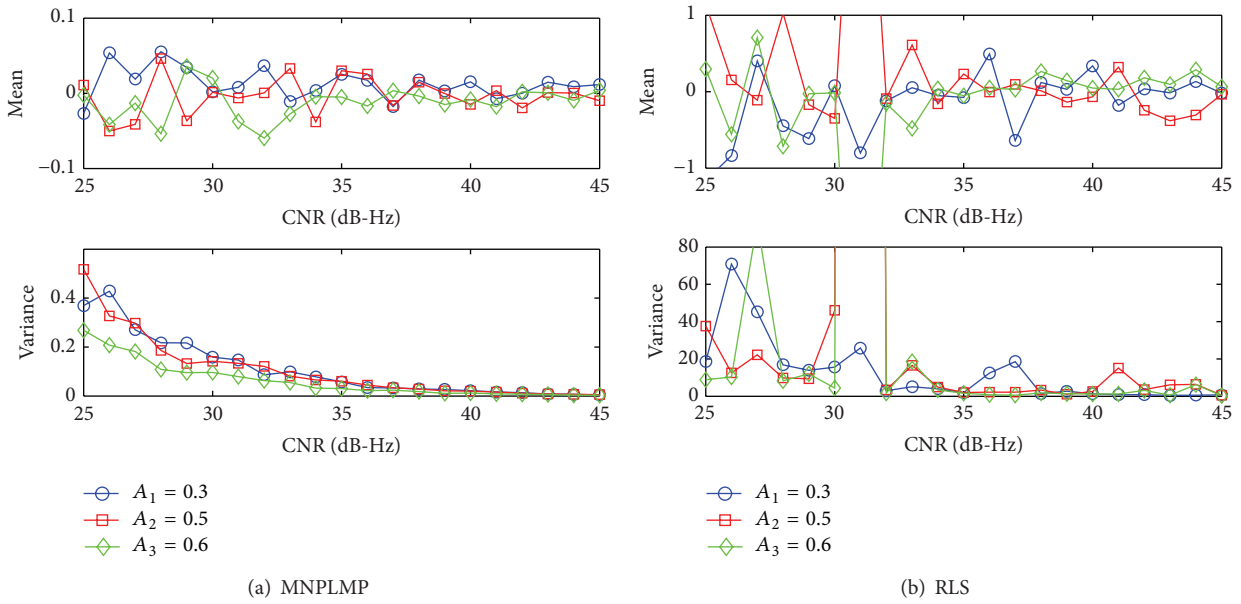

Figure 11: Multipath amplitude estimation errors in various CNRs under an impulsive noise environment.

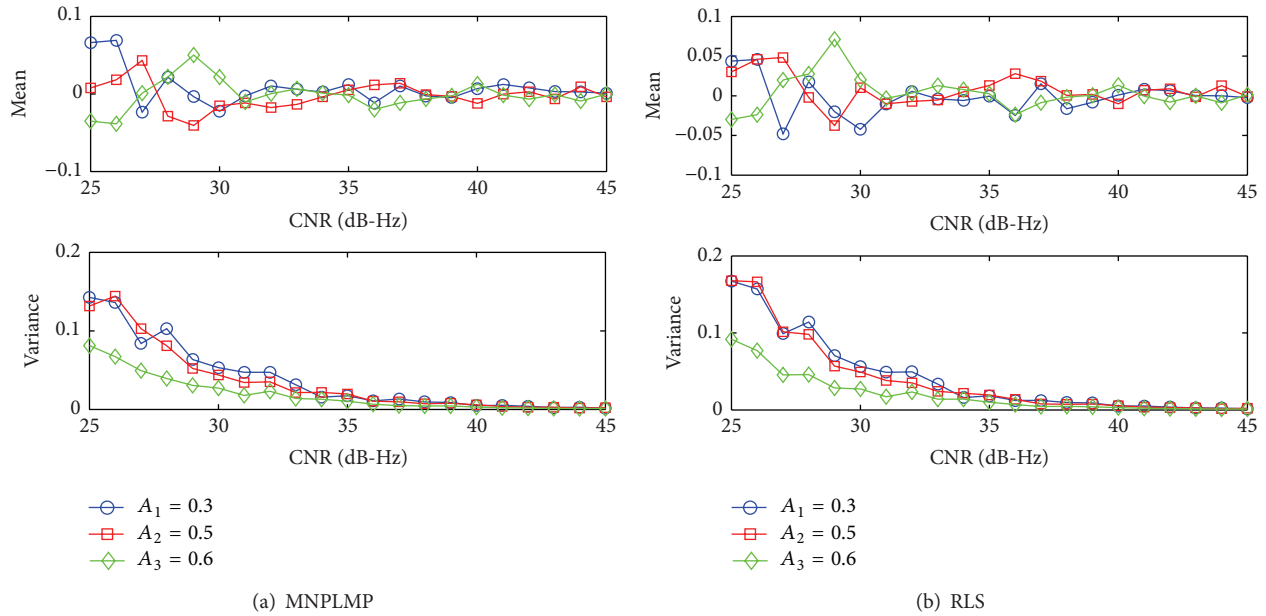

Figure 12: Multipath amplitude estimation errors in various CNRs under the AWGN environment.

chips; and the window width of the average filter was set to 20 ms. The estimation of each delay was used to compensate the correlator output. Moreover, the error of the compensated output was transferred to the range error. The obtained error envelopes in the two noise conditions were shown in Figure 13. To obtain the error envelope curves, negative multipath magnitude was also simulated though it had no special physical meaning.

The designed multipath mitigation scheme in both conditions was able to efficiently estimate and compensate for the corresponding delay (Figure 13). Furthermore, the compensation precision for the short-delay multipath was acceptable, and its error was less than 6 m. Because the code discriminator output was close to zero at around half of one chip, this position was sensitive to noise, and a larger error could be observed at 0.7 chips. In this case, narrow correlator spacing was usually adopted to achieve a higher compensation precision. References [6, 7] had demonstrated its superiority.

5. Conclusion

To obtain a faster convergence rate and higher processing gain in the presence of the impulsive noise condition, a BDS

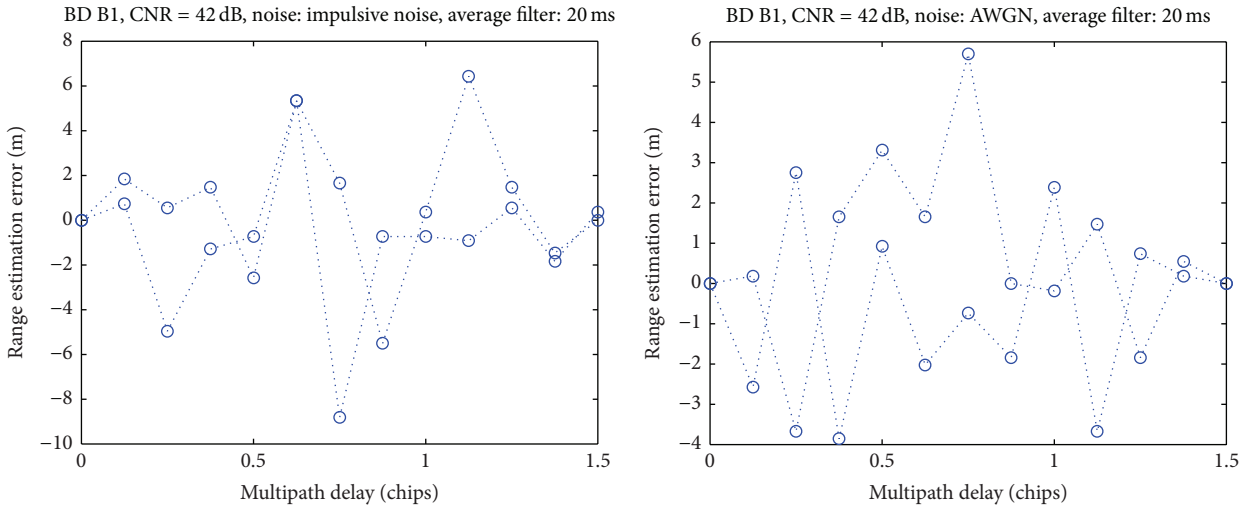

(a) Impulsive noise interference

(b) AWGN noise interference

Figure 13: The ranging estimation error after removing multipath.

short-delay multipath mitigation scheme with modified adaption algorithms and a simple average filter was designed.

For the modified adaption algorithms, the RLS algorithm does not suppress the impulsive noise mostly. Therefore, a better adaption algorithm was presented. The proposed scheme accelerates convergence rate of the traditional algorithm by introducing the weight-changing tendency term. Its steady-state error was similar to that of the traditional algorithm. Extended algorithms were also directly provided according to similar principle.

The comparative performance assessments in the normal and degraded conditions indicated that the proposed approach was suitable for estimating the multipath parameters under the impulsive and AWGN noise interference. Given a correlator spacing of 0.5 chips, the scheme's delay estimation error was less than 9 m for any delay and 6 m for short-delay. Consequently, a better effect was expected if the correlator spacing was decreased.

The average filter improved the processing gain with an acceptable performance on the critical value of 35 dB-Hz. However, this value was not enough for the CNRs below 35 dB-Hz. Further studies should be conducted.

Conflict of Interests

The authors declare that there is no conflict of interests regarding the publication of this paper.

Acknowledgments

The financial support from the National Science Foundation of China under Grant (nos. 61304234 and 61273081) and the Fundamental Research Funds for the Central Universities (HEUCFX041403 and HEUCFR1114) are gratefully acknowledged.

References

[1] http://www.beidou.gov.cn/.

[2] J. M. Sleewaegen and F. Boon, "Mitigating short-delay multipath: a promising new technique," in *Proceedings of the 14th International Technical Meeting of the Satellite Division of the Institute of Navigation (ION GPS '01)*, pp. 204–213, Salt Lake City, Utah, USA, September 2001.

[3] J.-A. Wang, P.-J. Liu, and S.-S. Li, "An adaptive genetic algorithm for complex close-in Galileo BOC(1, 1) multipath mitigation," *Journal of Central South University (Science and Technology)*, vol. 43, no. 12, pp. 4757–4763, 2012 (Chinese).

[4] W.-L. Mao, J.-S. Du, J. Sheen, and C.-S. Hwang, "Adaptive multipath mitigation tracking system for GPS receiver," *Aerospace Science and Technology*, vol. 30, no. 1, pp. 66–78, 2013.

[5] M. Rlinami, H. Morikawa, and T. Aoyama, "Adaptive multipath mitigation technique for GPS signal reception," in *Proceedings of the 51st Vehicular Technology Conference (VTC '00)*, pp. 1625–1629, May 2000.

[6] C.-L. Chang and J.-C. Juang, "An adaptive multipath mitigation filter for GNSS applications," *EURASIP Journal on Advances in Signal Processing*, vol. 2008, Article ID 214815, 10 pages, 2008.

[7] Y. Zhao, X. Xue, and T. Zhang, "Receiver-channel based adaptive blind equalization approach for GPS dynamic multipath mitigation," *Chinese Journal of Aeronautics*, vol. 26, no. 2, pp. 378–384, 2013.

[8] L. Liu and M. G. Amin, "Performance analysis of GPS receivers in non-Gaussian noise incorporating precorrelation filter and sampling rule," *IEEE Transactions on Signal Processing*, vol. 56, no. 3, pp. 990–1004, 2008.

[9] J. Arribas, C. Fernández-Prades, and P. Closas, "Array-based GNSS acquisition in the presence of colored noise," in *Proceedings of the 36th IEEE International Conference on Acoustics, Speech, and Signal Processing (ICASSP '11)*, pp. 2728–2731, Prague Congress Center, Prague Czech Republic, May 2011.

[10] M. D. Button, J. G. Gardiner, and I. A. Glover, "Measurement of the impulsive noise environment for satellite-mobile radio

systems at 1.5 GHz," *IEEE Transactions on Vehicular Technology*, vol. 51, no. 3, pp. 551–560, 2002.

[11] S. Yoon, I. Song, and S. Y. Kim, "Code acquisition for DS/SS communications in non-Gaussian impulsive channels," *IEEE Transactions on Communications*, vol. 52, no. 2, pp. 187–190, 2004.

[12] C. L. Nikias and Shao M., *Signal Processing with Alpha-Stable Distributions and Applications*, Wiley-Interscience, New York, NY, USA, 1995.

[13] P. G. Georgiou, "Alpha-stable modeling of noise and robust timedelay estimation in the presence of impulsive noise," *IEEE Transactions on Multimedia*, vol. 1, no. 3, pp. 291–301, 1999.

[14] I. Hacıoglu, F. K. Harmancı, E. Anarım et al., "Time-of-arrival estimation under impulsive noise for wireless positioning systems," in *Proceedings of the 14th European Signal Processing Conference (EUSIPCO '06)*, pp. 1–5, Florence, Italy, September 2006.

[15] L. R. Vega, H. Rey, J. Benesty, and S. Tressens, "A new robust variable step-size NLMS algorithm," *IEEE Transactions on Signal Processing*, vol. 56, no. 5, pp. 1878–1893, 2008.

[16] Y. Li, W. Li, W. Yu, J. Wan, and Z. Li, "Sparse adaptive channel estimation based on l_p-norm-penalized affine projection algorithm ," *International Journal of Antennas and Propagation*, vol. 2014, Article ID 434659, 8 pages, 2014.

[17] M. Shao and C. L. Nikias, "Signal processing with fractional lower order moments: stable processes and their applications," *Proceedings of the IEEE*, vol. 81, no. 7, pp. 986–1010, 1993.

[18] O. Arikan, A. E. Cetin, and E. Erzin, "Adaptive filtering for non-Gaussian stable processes," *IEEE Signal Processing Letters*, vol. 1, no. 11, pp. 163–165, 1994.

[19] L. Jacek, *Signal processing in stable noise environments [Doctoral thesis]*, Department of Engineering University of Cambridge, 1998.

[20] Y. R. Zheng and T. Shao, "A variable step-size LMP algorithm for heavy-tailed interference suppression in phased array radar," in *Proceedings of the IEEE Aerospace Conference*, pp. 1–6, Big Sky, Mont, USA, March 2009.

[21] BeiDou navigation satellite system signal in space interface control document [Test Version], 2013, http://www.beidou.gov.cn/.